The Plant Cell, Vol. 24: 1034–1048, March 2012, www.plantcell.org

Genetic Control of Seed Shattering in Rice by the APETALA2 Transcription Factor *SHATTERING ABORTION1* [C][W][OA]

Yan Zhou,[a,1] Danfeng Lu,[a,1] Canyang Li,[a] Jianghong Luo,[a] Bo-Feng Zhu,[a] Jingjie Zhu,[a] Yingying Shangguan,[a] Zixuan Wang,[a,b] Tao Sang,[c] Bo Zhou,[d] and Bin Han[a,e,2]

[a] National Center for Gene Research, National Center for Plant Gene Research (Shanghai) and Institute of Plant Physiology and Ecology, Shanghai Institutes for Biological Sciences, Chinese Academy of Sciences, Shanghai 200233, China
[b] Plant Genome Center, Tsukuba, Ibaraki 305-0856, Japan
[c] State Key Laboratory of Systematic and Evolutionary Botany, Key Laboratory of Plant Resources, Institute of Botany, Chinese Academy of Sciences, Beijing 100093, China
[d] Zhejiang Academy of Agricultural Sciences, Hangzhou 310021, China
[e] Beijing Institute of Genomics, Chinese Academy of Sciences, Beijing 100029, China

Seed shattering is an important agricultural trait in crop domestication. *SH4* (for grain shattering quantitative trait locus on chromosome 4) and *qSH1* (for quantitative trait locus of seed shattering on chromosome 1) genes have been identified as required for reduced seed shattering during rice (*Oryza sativa*) domestication. However, the regulatory pathways of seed shattering in rice remain unknown. Here, we identified a seed *shattering abortion1* (*shat1*) mutant in a wild rice introgression line. The *SHAT1* gene, which encodes an APETALA2 transcription factor, is required for seed shattering through specifying abscission zone (AZ) development in rice. Genetic analyses revealed that the expression of *SHAT1* in AZ was positively regulated by the trihelix transcription factor *SH4*. We also identified a frameshift mutant of *SH4* that completely eliminated AZs and showed nonshattering. Our results suggest a genetic model in which the persistent and concentrated expression of active *SHAT1* and *SH4* in the AZ during early spikelet developmental stages is required for conferring AZ identification. *qSH1* functioned downstream of *SHAT1* and *SH4*, through maintaining *SHAT1* and *SH4* expression in AZ, thus promoting AZ differentiation.

INTRODUCTION

Seed shattering is an adaptive trait for seed dispersal in wild plants. However, the seed shattering habit causes yield loss for domesticated crop plants during harvest. Our ancestors began domesticating crop plants by selecting grains that had reduced seed shattering characteristics (Doebley, 2006; Fuller et al., 2009). Seed shattering occurs in the anatomically distinct cell files known as the abscission zone (AZ). Differentiated AZ cells are small, isodiametric, and cytoplasmically dense compared with surrounding cells and are responsive to signals promoting abscission (Hoekstra et al., 2001; Jin, 1986; McKim et al., 2008; Szymkowiak and Irish, 1999). Often these signals are associated with the senescence of the distal organ. However, a spectrum of environmental factors, such as a deficit or surplus of water, extremes of temperature, or pest and pathogen attack, can prematurely precipitate leaf, flower, or fruit fall (Taghizadeh et al., 2009; Taylor and Whitelaw, 2001). Understanding how the process of abscission is regulated in model crops would benefit agriculture.

Previous studies of rice (*Oryza sativa*) have identified a few of the factors involved in seed shattering. *SH4* is a member of the trihelix family of transcription factors and promotes hydrolyzing of AZ cells during the abscission process (Li et al., 2006; Lin et al., 2007). The cultivated rice allele of *sh4* severely weakens but does not eliminate shattering (Li et al., 2006). *qSH1*, a major rice quantitative trait locus on chromosome 1, encodes a BEL1-type homeobox-containing protein. A single nucleotide polymorphism (SNP) in the 5′ upstream regulatory region of *qSH1* causes *qSH1* expression to disappear from the abscission layer, thus leading to a decline in seed shattering over the history of rice domestication (Konishi et al., 2006). Recently, a recessive shattering locus *sh-h*, encoding a C-terminal domain phosphatase-like protein, was identified using mutagenesis of cultivated rice and was shown to inhibit the development of AZs in rice (Ji et al., 2010). In addition to the three rice shattering genes, the wheat (*Triticum turgidum*) *Q* gene was reported to affect the compaction and fragility of wheat ears and also the ease with which the grain can be separated from the chaff (Doebley, 2006; Simons et al., 2006). *Q* is a member of the APETALA2 (AP2) family of transcription factors, which have been implicated in a wide variety of plant development roles.

There is a wide range in the degree of seed shattering among worldwide rice cultivars (Konishi et al., 2006), suggesting that the shattering habit is a polygenic and complex trait. To better understand the process of seed abscission and exploit the network of different genes regulating the rice shattering pathway, we

[1] These authors contributed equally to this work.
[2] Address correspondence to bhan@ncgr.ac.cn.
The author responsible for distribution of materials integral to the findings presented in this article in accordance with the policy described in the Instructions for Authors (www.plantcell.org) is: Bin Han (bhan@ncgr.ac.cn).
[C]Some figures in this article are displayed in color online but in black and white in the print edition.
[W]Online version contains Web-only data.
[OA]Open Access articles can be viewed online without a subscription.
www.plantcell.org/cgi/doi/10.1105/tpc.111.094383

investigated suppressor mutants in a genetic background containing known seed shattering–related genes in which the shattering events have in some way been impaired. To this end, we constructed a shattering chromosomal segment substitution line (CSSL), Substitution Line 4 (SL4), by introducing chromosome 4 of wild-rice *Oryza rufipogon* W1943 (easy shattering) into the recurrent parent *O. sativa* ssp *indica* cv Guangluai 4 (GLA4) (reduced shattering). We identified a number of new nonshattering rice mutants by ^{60}Co γ-ray mutagenesis of SL4.

In this study, we report the isolation and characterization of one of these nonshattering mutants, *shattering abortion1* (*shat1*). By map-based cloning, we identified the AP2 domain–containing transcription factor gene *SHAT1* as responsible for AZ development. We also identified a new allelic mutant of *SH4* that showed a complete loss-of-shattering phenotype, differing from the reduced-shattering habit that results from the *sh4* allele in cultivated rice. Genetic analyses demonstrated that *SH4* plays a role early in AZ differentiation, and the expression of *SHAT1* in the AZ was positively regulated by *SH4*. We also show that *qSH1* functions downstream of *SHAT1* and *SH4* to maintain their expression in the AZ, thus promoting AZ differentiation. Our results suggest a genetic model in which the persistent and concentrated expression of the active *SHAT1* and *SH4* in the AZ during early spikelet developmental stages is required for conferring AZ identification.

RESULTS

Characterization of Two Nonshattering Mutants in Rice

To explore the seed shattering regulation pathways, we constructed a CSSL by introgressing chromosome 4 of the shattering donor parent *O. rufipogon* W1943 into the reduced-shattering recurrent parent *O. sativa* ssp *indica* cv GLA4 (Zhu et al., 2011) (see Supplemental Figures 1A and 1B online). This chromosome 4 substitution line was designated as the SL4. SL4 exhibited a very easy shattering phenotype as a result of not only acquiring *SH4* from wild rice but also harboring *qSH1* in the *indica* genetic background. SL4 is also referred to as the wild type below. We then generated a rice mutant library by treating the shattering seeds of SL4 with ^{60}Co γ-rays and screened for nonshattering mutants among the T1 plants, isolating two mutant lines (Figure 1A): We named these *shat1* and *shat2*, respectively.

In addition to loss of shattering, the *shat1* mutant displayed a range of spikelet and inflorescence developmental defects, including (1) palea degeneration or florets with multiple layers of lemma- and palea-like structures (see Supplemental Figures 2A to 2D and 3H online); (2) changes in numbers, size, appearance, and identities of floral organs, especially carpels and anthers (see Supplemental Figures 2I to 2K and 3D to 3G online); (3) longer grains (see Supplemental Figure 3A online); (4) fewer primary branches (see Supplemental Figure 3B online); and (5) reduced seed set rate (see Supplemental Figure 3C online). Notably, the *shat1* mutant displayed a unique phenotype of a crook-neck-like rachilla between the sterile lemmas and the rudimentary glumes in the position where the AZ was usually formed (Figures 1C, 1D, 1I, and 1J). In contrast with *shat1*, the *shat2* mutant showed no significant morphological alterations in spikelets, except for the shattering defect and smaller seeds (Figures 1O and 1P; see Supplemental Figures 2E, 2L, 4A, and 4B online). The *shat1 shat2* double mutant had a crook-neck-like rachilla (Figures 1U and 1V; see Supplemental Figure 2F online) and showed similar spikelet defects to those in *shat1*, including aberrant palea, lemma, and inner floral organs (see Supplemental Figures 2G, 2H, 2M, and 2N online).

Disruption of AZ Results in a Nonshattering Phenotype in the *shat1* and *shat2* Mutants

The shattering defect of *shat1* and *shat2* mutant was further characterized by measuring pedicel breaking tensile strength (BTS), which is inversely proportional to shattering degree. During the first 6 d after pollination, the BTS force did not differ between the developmental stages in either line (Figure 1B). From 11 d, the BTS value quickly decreased in the wild type. These changes may be due to the progressive degradation of the middle lamellae in the AZ. The BTS value decreased with maturating of seeds. By 13 d, shattering prevailed in the wild type, which left few grains to measure. In *indica* cv GLA4, the BTS began to decrease from 9 d. The earlier commencement of the decrease in GLA4 might be due to the faster maturating of seeds. However, the decline proceeded at a slower rate in GLA4 than in the wild type. From 9 d onward, the BTS showed no appreciable change in GLA4, and the values were about one-third of those displayed at the earlier stages but did not reach a level permitting grain shattering (Figure 1B). By contrast, neither *shat1* nor *shat2* mutants showed decreases in BTS with maturating of seeds, suggesting that cell wall adhesion at the seed-pedicel junction did not weaken in these two mutants (Figure 1B). The *shat1 shat2* double mutant showed similar changes in BTS values to those in *shat1* during seed development.

To distinguish precisely the differences in AZ anatomy among *shat1*, *shat2*, and the wild type, longitudinal sections of spikelets at anthesis stage were compared using confocal microscopy. Isodiametrically flattened and thin-walled AZ cells were visible in the basal area near sterile lemmas in the wild type (Figures 1E and 1F). GLA4, however, had an incomplete abscission layer; in the longitudinal section, the line of abscission cells was discontinuous and completely absent near the vascular bundle, where they were replaced by thick-walled cells similar to adjacent pedicel cells (see Supplemental Figure 5A online). In the *shat1* (Figures 1K and 1L) and *shat1 shat2* mutants (Figures 1W and 1X), such a layer of abscission cells was substituted by peanut-like, thick-walled cortical cells. In the *shat2* mutant, although AZ cells had a small and flattened appearance, they were not thin walled, as their cell walls were stained green by Acridine Orange, an indicator for lignin deposition when excited with a 488-nm laser (Briggs and Morris., 2008) (Figures 1Q and 1R). These results suggest that a cytologically distinct and active seed AZ is not properly formed in both *shat1* and *shat2* mutants.

We then used scanning electron microscopy to examine the interface where a mature grain separates from the pedicel. Consistent with the BTS testing results, there was a smooth fracture surface of rachilla in the wild type as a result of hydrolyzing of the middle lamellae during the seed shattering process

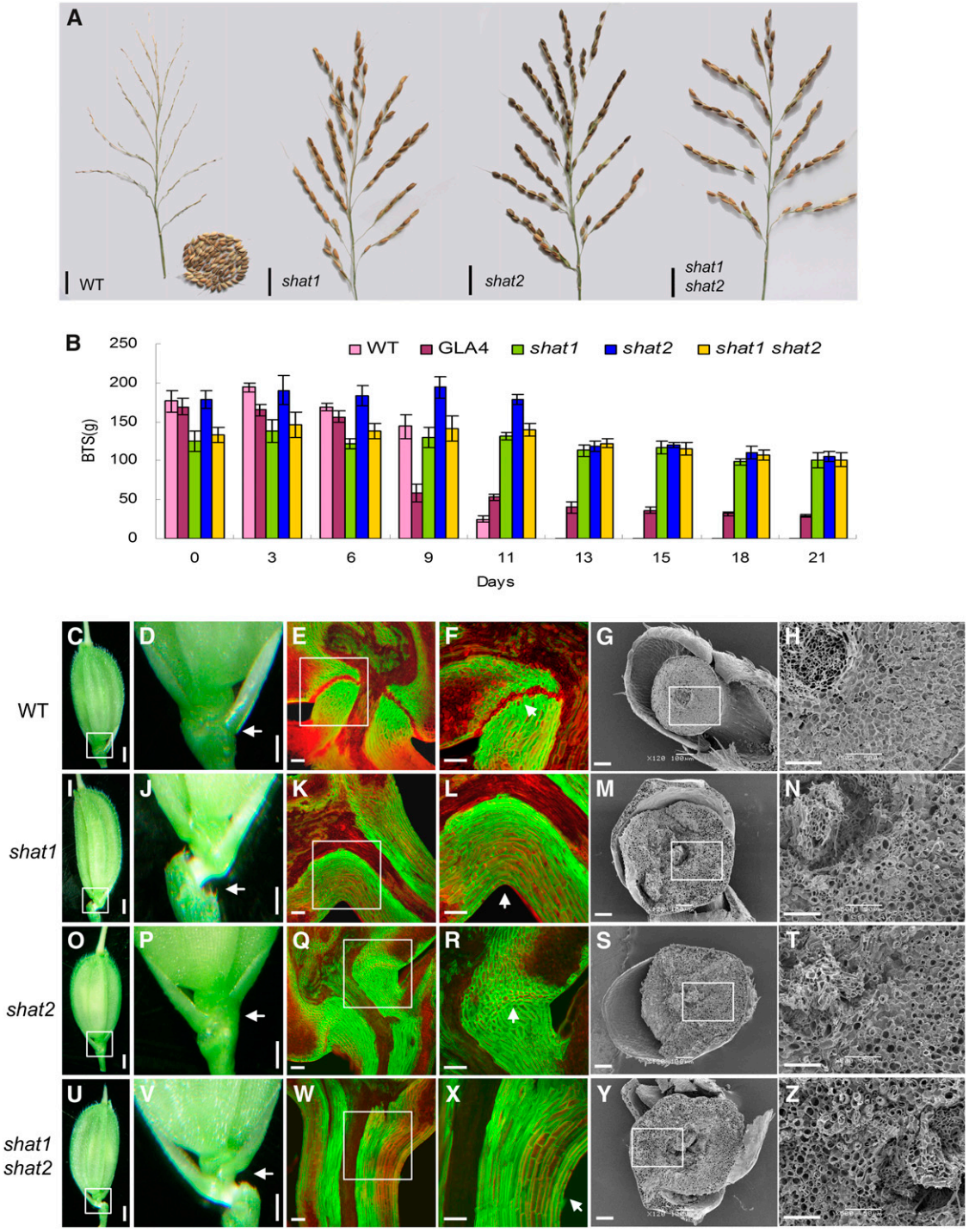

Figure 1. Characterization of Seed Shattering and Floral AZ Morphology in Wild Type and Different Mutant Lines.

(A) Bagged panicles harvested from wild-type (WT; SL4), *shat1* mutant, *shat2* mutant, and *shat1 shat2* double mutant plants when seeds were fully ripened. Right corner in the wild-type photo shows the automatically shattering seeds collected in the bag. Bars = 1 cm.

(B) Force required to pull flowers or grains off of pedicels of the wild type, *shat1* mutant, *shat2* mutant, and *shat1 shat2* double mutant on the day of flower opening (0) and every 3 or 2 d thereafter during seed development. Error bars, ±SD.

(C) to **(Z)** Morphological characteristics of AZs. The four rows from top to bottom represent morphological analyses of the wild type, *shat1* mutant, *shat2* mutant, and *shat1 shat2* double mutant, respectively. **(C)**, **(I)**, **(O)**, and **(U)** show the spikelets. The white boxes indicate the region where AZ is located. Bars = 1 mm. **(D)**, **(J)**, **(P)**, and **(V)** show close-up views corresponding to the white boxes in **(C)**, **(I)**, **(O)**, and **(U)**, respectively. Arrows indicate the

(Figures 1G and 1H). Moreover, the fracture surface of the retained rachilla in the wild type was filled with callose that might serve as an ideal barrier to resist pathogen invasion (Figure 1H). In GLA4, the outer surface was smooth, while the center surface was rough, consistent with its discontinuous AZs (see Supplemental Figure 5B online). In *shat1* (Figures 1M and 1N), *shat2* (Figures 1S and 1T), and *shat1 shat2* mutants (Figures 1Y and 1Z), external force was needed to remove seed from the pedicels when seeds were fully ripened and this left a rough and irregular surface.

SHAT1 Encodes an AP2-Like Transcription Factor, and a Frameshift in the *SHAT2* Locus Completely Disrupts *SH4* Function

A map-based cloning approach was adopted to isolate the corresponding *SHAT1* and *SHAT2* genes associated with the mutations in the *shat1* and *shat2* mutants, respectively. Genetic crossing indicated they were nonallelic mutants. In addition, *shat1* was also not allelic to the known shattering genes *sh4* and *qSH1*. As the crook-neck-like rachilla was a typical and visible phenotype resulting from loss of AZ for the *shat1* mutant, we therefore adopted it as a standard *shat1* phenotype (Figure 1J). All F1 progeny deriving from the cross between *shat1* and the wild type showed the same phenotypes of seed shattering as wild-type plants and without the crook-neck-like rachilla. In the F2 population, shattering and nonshattering plants segregated in a 3:1 ratio (314:104, n = 1, χ^2 = 0.006, P = 0.936), and the nonshattering phenotype cosegregated with crook-neck-like rachilla, indicating that a single recessive locus was the cause of these two phenotypes in *shat1*. For the construction of a mapping population, the *shat1* mutant was crossed with the *japonica* cv Nipponbare. A total of 300 F2 plants that had crook-neck-like rachilla were selected for mapping analysis. *SHAT1* was initially mapped on the long arm of chromosome 4 between the two insertion or deletion (indels) markers M1056 and M6026 and was subsequently fine-mapped to a 9.0-kb interval between two SNP markers, A and B (Figure 2A; see Supplemental Table 1 online). In this candidate region, only one gene, which encoded an AP2 transcription factor (LOC_Os04g55560) with a 459-residue polypeptide protein, was annotated in The Institute for Genomic Research Rice Genome Annotation database (http://rice.plantbiology.msu.edu/; Figure 2B). Comparison of the nucleotide sequences of the candidate gene in *shat1* mutant and wild-type plants revealed a 1-bp deletion in the first exon between the nucleotide sites +41 and +42 in the *shat1* mutant, resulting in a frameshift (Figure 2B). A homology search by BLASTP found that the SHAT1 is a rice ortholog of the *Arabidopsis thaliana* AP2 protein (Figure 2C), which was shown to be involved in the regulation of flower development (Chen., 2004; Wollmann et al., 2010).

SHAT2 was first mapped on the long arm of chromosome 4 in a 1000-kb region using the F2 population crossed with *japonica* cv Nipponbare (Figure 2D). We then used another F2 population crossed with *indica* cv GLA4 for fine mapping the *SHAT2*. The *SHAT2* locus was finally narrowed down to a 9.7-kb region that encompassed two predicted genes (Figure 2D). Comparison of the 9.7-kb sequences between the wild type and *shat2* mutant revealed a one-nucleotide insertion in the second exon of the first gene, which was known to be *SH4* (LOC_Os04g57530; Figure 2E). Differing from the one–amino acid substitution in cultivated rice *sh4* allele, the *shat2* mutation resulted in a frameshift before the nuclear localization signal region (Figure 2F). To distinguish these two different *sh4* mutant alleles, we renamed the *sh4* allele in cultivated rice as *sh4-1* and the *shat2* allele as *sh4-2* in the following text.

Genetic Analysis Confirms that the *SHAT1* Affects Rice Seed Shattering

As the *shat1* mutant has both *indica* and wild rice genetic backgrounds, it failed to regenerate shoots from callus. Thus, we could not directly perform a complementation test to identify the function of *SHAT1* in the *shat1* mutant line. To verify the responsibility of *SHAT1* in specifying the AZ, we generated a *SHAT1*-RNA interference (RNAi) construct (Figure 3A) and transformed it into the *indica* cv Kasalath, which possesses the wild-type allele of *SHAT1* and has a reduced-shattering phenotype. Eight independent *SHAT1*-RNAi T0 transgenic plants showed various degrees of increased BTS values compared with Kasalath, and these values correlated well with the magnitude of the reduction in *SHAT1* mRNA (Figure 3B). Two RNAi lines (lines 2 and 8) with varied levels of suppression were used for AZ anatomical structure studies: Line 8 had a stronger defective AZ phenotype than line 2 (Figure 3C). This observation was consistent with the results that line 8 contained ~17%, while line 2 contained ~51% of the wild-type *SHAT1* mRNA levels (Figure 3B).

More evidence supporting the involvement of *SHAT1* in AZ development was obtained from the characterization of another allelic *SHAT1* mutant line (2B70080) identified in the T-DNA (T-DNA) insertion line database (Jeon et al., 2000). This mutant line had a T-DNA insertion in the 3′ untranslated region (UTR) of *SHAT1* (Figures 3D and 3E). The expression levels of *SHAT1* were dramatically decreased in mutant 2B70080 compared with its wild-type *japonica* cv Huayong. This result also correlated closely with the increasing BTS value in 2B70080 (Figure 3F). Further investigation of the AZ anatomical structure using

Figure 1. (continued).

position of AZ. Bars = 0.5 mm. **(E)**, **(K)**, **(Q)**, and **(W)** show fluorescence images of longitudinal sections across flower and pedicel junction stained by Acridine Orange. The white boxes indicate the region where AZ is located. Bars = 50 μm. **(F)**, **(L)**, **(R)**, and **(X)** show close-up views corresponding to the white boxes in **(E)**, **(K)**, **(Q)**, and **(W)**, respectively. Arrows point to the AZ in the wild type or the corresponding region in mutant lines. Bars = 50 μm. **(G)**, **(M)**, **(S)**, and **(Y)** show scanning electron microscopy photos of the pedicel junction after detachment of seeds. Bars = 100 μm. The white boxes contain the outer and the center region on the surface. **(H)**, **(N)**, **(T)**, and **(Z)** show close-up scanning electron microscopy photos corresponding to the white boxes in **(G)**, **(M)**, **(S)**, and **(Y)**. Peeled-off and smooth surfaces are observed in the wild type **(H)**, whereas broken and rough surfaces are observed in *shat1* **(N)**, *shat2* **(T)**, and *shat1 shat2* **(Z)**. Bars = 50 μm.

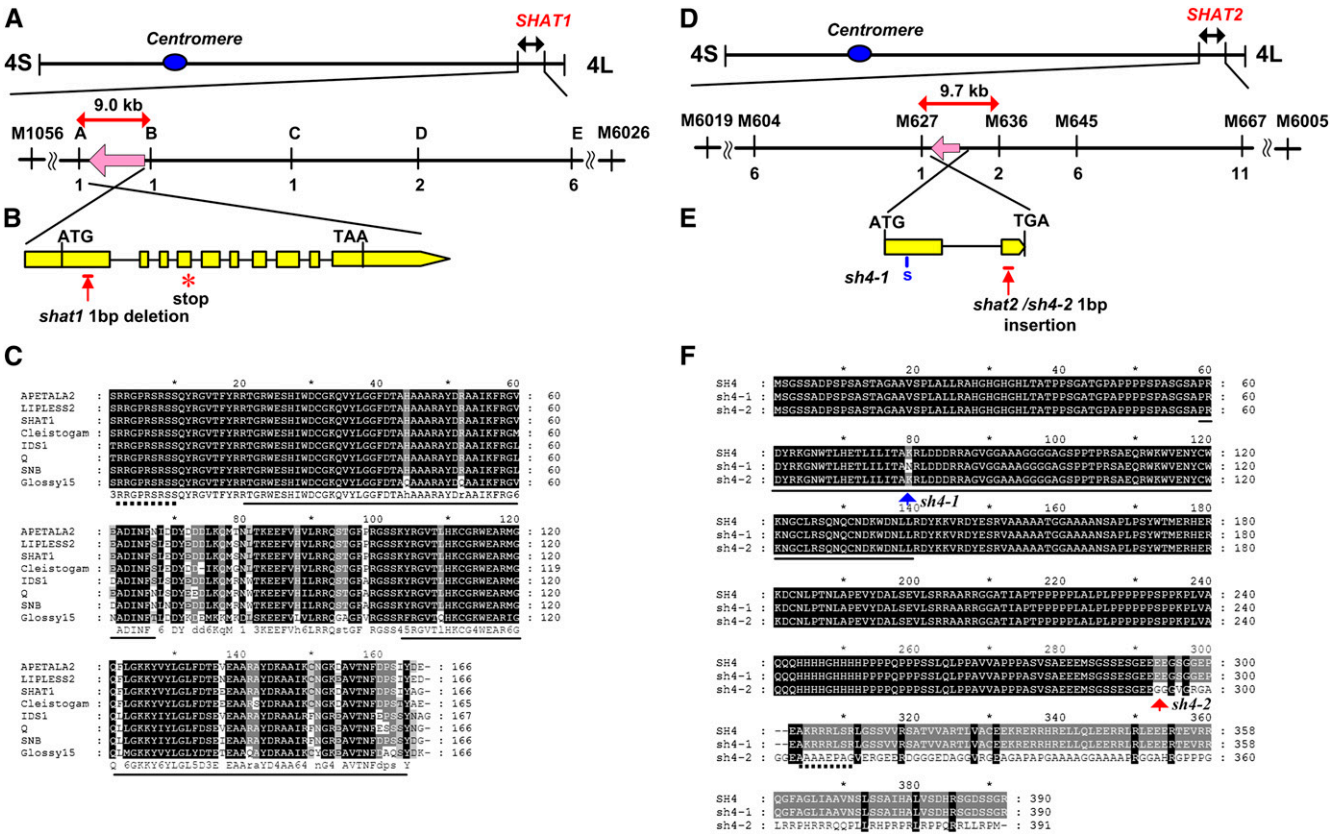

Figure 2. Map-Based Cloning of *SHAT1* and *SHAT2*.

(A) Fine-mapping of the *SHAT1* locus. The *SHAT1* locus was narrowed down to a 9-kb region between markers A and B on chromosome 4 using 300 homozygous F2 plants and is indicated by a pink arrow. Numbers below the horizontal line are the number of recombinants.

(B) Schematic representation of the *SHAT1* gene. Exons and introns are represented by yellow boxes and horizontal lines, respectively. The start codon (ATG) and stop codon (TAA) sites are indicated by vertical crossing lines. Location of the mutation site is indicated by a vertical arrow. The red star indicates the site of a premature stop codon caused by the 1-bp deletion.

(C) Amino acid sequence alignments of the AP2 domain. AP2 domain regions are underlined. The putative nuclear localizing signal region is underlined with a dotted line. Black and gray shading indicate 100 and 80% conserved amino acid residues, respectively. The names of protein are indicated on the left.

(D) Fine-mapping of the *SHAT2* locus. The *SHAT2* locus was narrowed down to a 9.7-kb region between markers M627 and M636 using 907 homozygous F2 plants and is indicated by a pink arrow. Numbers below the horizontal line are the number of recombinants.

(E) *SHAT2* structure. Two exons and one intron are represented by yellow boxes and a horizontal line, respectively. The mutation sites in *sh4-1* and *sh4-2* are indicated by a blue vertical line and a red vertical arrow, respectively. The blue S indicates the site of a 1-bp substitution in *sh4-1*, and a short horizontal red line indicates the site of a 1-bp insertion in *sh4-2*.

(F) The amino acid sequence comparison of *SH4*, *sh4-1*, and *sh4-2*. Trihelix DNA binding domain regions are underlined. The putative nuclear localizing signal region is underlined with a dotted line. Arrows indicate the mutation site in *sh4-1* (blue) and *sh4-2* (red).

[See online article for color version of this figure.]

confocal microscopy indicated that the thin-walled property of AZ cells was altered in the 2B70080 mutant (Figure 3G). Overall, these results confirmed that the loss of shattering in the *shat1* mutant was caused by disruption of the *SHAT1* gene.

SHAT1 Is Localized in the Nucleus and Has Transactivational Activity

SHAT1 protein was predicted to have a nuclear localization signal by the PSORT program (http://psort.hgc.jp/). To confirm this prediction, we made a construct constitutively expressing the full-length SHAT1 fused to the C terminus of green fluorescent protein (GFP). We transiently expressed the SHAT1-GFP fusion protein in onion epidermal cells and observed GFP signal to be exclusively localized in the nucleus (see Supplemental Figure 6 online).

Although SHAT1 acts as a transcription factor and is localized in the nucleus, it is unknown whether SHAT1 has transcriptional activation activity. We applied the yeast one-hybrid system to detect transcriptional activation activity of SHAT1. The yeast GAL4 DNA binding domain was fused to different segments of

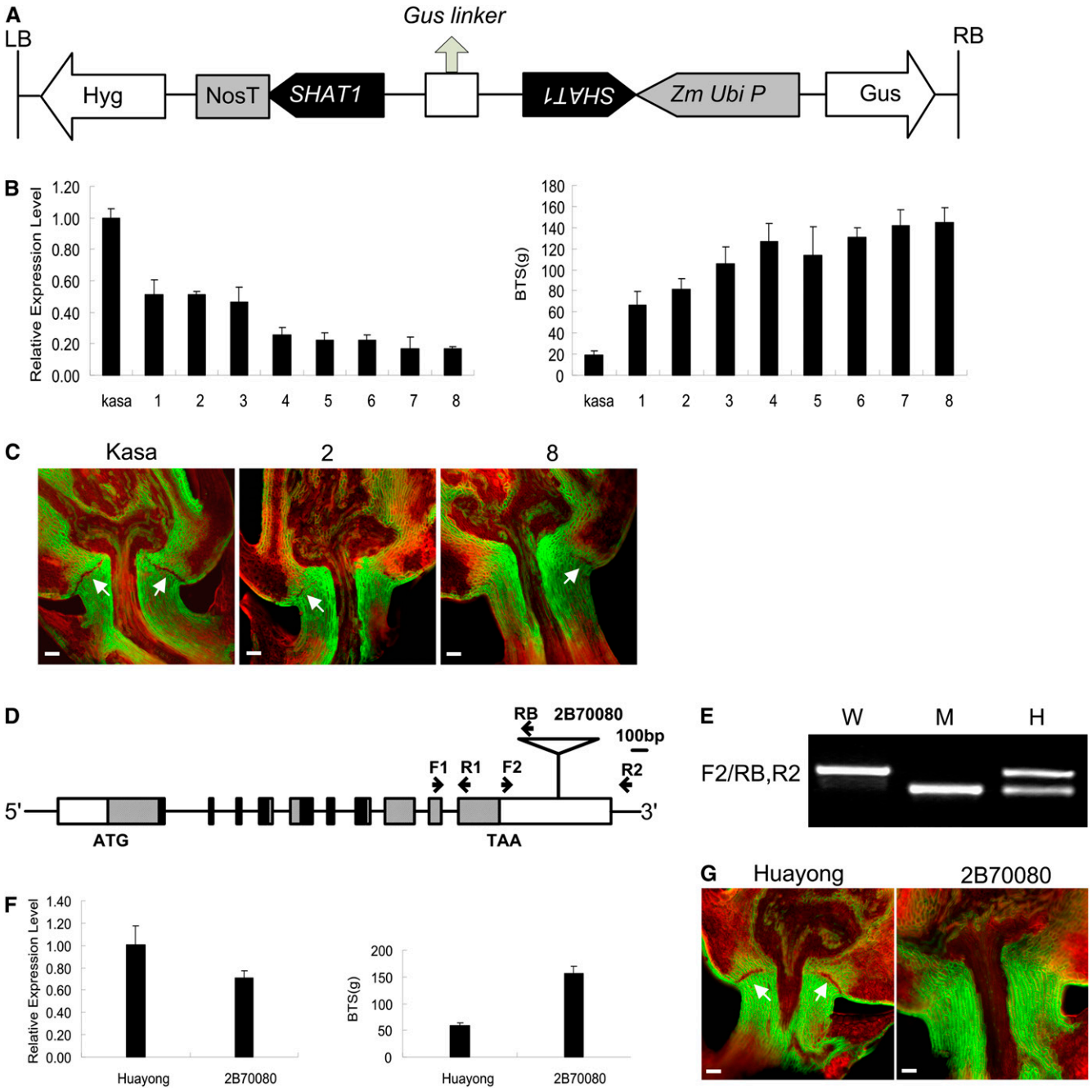

Figure 3. Genetic Identification of *SHAT1*.

(A) Schematic diagram of *SHAT1* RNAi construct. A 426-bp cDNA fragment around the stop codon was used to generate the *SHAT1*-RNAi construct in the pTCK303 vector. Hyg, hygromycin-resistant gene; LB and RB, left and right borders, respectively; NosT, nopaline synthase terminator; *SHAT1*, a 426-bp *SHAT1* cDNA fragment; Zm Ubi P, maize (*Zea mays*) *ubiquitin* promoter.

(B) Corresponding relationship between *SHAT1* expression profiles and shattering degree in the control plant Kasalath (Kasa) and eight *SHAT1*-RNAi transgenic plants. Left: Relative expression of *SHAT1* revealed by real-time RT-PCR using RNA isolated from panicles on the day of flowering. Error bars indicate ± SD of the mean of three biological samples. Right: Force required to pull off seeds from pedicels at 30 d after flowering when seeds were fully ripened. Error bars indicate ± SD.

(C) Longitudinal sections across AZ of Kasalath and RNAi transgenic plants. Arrows indicate the AZ. Bars = 50 μm.

(D) Schematic diagram of a T-DNA mutant line, 2B70080. Gray boxes indicate coding regions, black boxes indicate AP2 domains, and white boxes show the 5′ and 3′ UTRs. The triangle represents the T-DNA, which was inserted into the 3′ UTR. Primers F1 and R1 were used for quantitative real-time RT-PCR analyses of *SHAT1* transcript levels. F2, RB, and R2 were used for mapping the T-DNA insertion.

SHAT1 (Figure 4). The full-length of rice bZip72 was used as a positive control (Lu et al., 2009). All transformants grew well on synthetic dropout (SD) medium lacking Trp (Figure 4). Then, yeast colonies of each transformant were transferred onto either Trp- and adenylate (Ade)-negative SD media or Trp- and His (His)-negative SD media with 0.5 mM 3-amino-1,2,4-triazole (3AT), respectively. On the SD/Trp-/Ade- plate, all types of transformants failed to grow, except for the positive control. However, on the SD/Trp-/His- plate, transformants of the positive control, pGBKT7-SHAT1 and pGBKT7-SHAT1ΔC, grew well, whereas pGBKT7-SHAT1ΔN and the negative control displayed cell growth inhibition (Figure 4). These results revealed that the N terminus of SHAT1 peptide that included the AP2 domain exhibited weak transactivational activity.

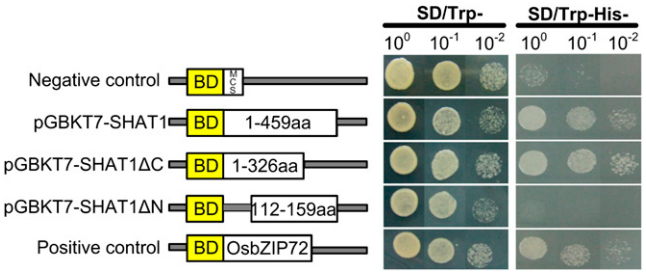

Figure 4. Transactivation Tests of SHAT1 in Yeast.

The constructs of the plasmids pGBKT7-SHAT1, pGBKT7-SHAT1ΔC, and pGBKT7-SHAT1ΔN are shown on the left. pGBKT7 was used as a negative control, and the known transcription factor Os-bZIP72 was fused with GAL4 BD of pGBKT7 as the positive control. Transactivation analysis of corresponding constructs by yeast one-hybrid was detected on the SD/Trp- and SD/Trp-/His-/0.5 mM 3AT media. GAL4 BD, GAL4 DNA binding domain; MCS, multiple cloning sites.
[See online article for color version of this figure.]

SHAT1 Is Universally Expressed in Tissues from Seedlings to Booting Panicle

We examined the expression pattern of *SHAT1* using quantitative RT-PCR and the β-glucuronidase (GUS) reporter gene under the control of the *SHAT1* promoter. *SHAT1* transcripts were universally present in all tested vegetative and reproductive tissues, from seedlings to the booting panicle by quantitative RT-PCR (Figure 5A). The GUS signal correlated well with the RT-PCR results. It was not only found in vegetative tissues, including leaf, stem, node, and leaf sheath (Figures 5B to 5E), but also in young spikelet (Figure 5F). In addition, *SHAT1* exhibited an intense signal in AZ and the inner floral organs of 2-mm-long spikelets (Figure 5G). When spikelet length was around 5 mm, GUS staining was weaker in the apiculus as well as in the palea and lemma (Figure 5H). With spikelet development, the GUS signals in spikelets gradually decayed (Figures 5I and 5J) and completely disappeared when spikelet length was around 8 mm.

The Expression of *SHAT1* in AZ Is Positively Regulated by *SH4*

To exploit the effect of *SHAT1* on AZ differentiation, we examined *SHAT1* expression during early floral development using in situ hybridization. The inflorescence and spikelet developmental stages used in this study were according to the criteria reported before (Itoh et al., 2005). Our analyses of *SHAT1* gene expression in the wild type showed that when lemma and palea primordia were first visible on the flanks of the floral meristem at sp6 stage, *SHAT1* mRNA showed hotspots of expression in palea and lemma primordia (Figure 6A; see Supplemental Figure 7A online). Subsequently, *SHAT1* signal declined in lemma and palea but appeared in the inner floral organ primordia, such as stamens and carpels during stage sp7, when carpel primordia began to differentiate (Figure 6B). When the ovule was first visible, *SHAT1* transcripts were restricted to the AZ and anthers from early stage sp8 (Figure 6C). Afterwards, during late sp8 stage, *SHAT1* expression accumulated to higher levels in the AZ than during early stage sp8 (Figure 6D). We also characterized *SHAT1* expression patterns in GLA4. Its genetic background is very close to the wild type, as mentioned above, but its *sh4-1* allele is the cultivated rice type. Therefore, we used GLA4 as the *sh4-1* mutant line in this study. The *SHAT1* signal in GLA4 was very similar to that in the wild type, showing converging expression in AZ from early stage sp8 and becoming more intense during late stage sp8 (Figures 6E to 6H). By contrast, the *sh4-2* mutation completely disrupted *SHAT1* expression in AZ, with no signals observed during stages sp6-sp8 (Figures 6I to 6L), similar to that in the *shat1* mutant (Figures 6M to 6P).

The altered expression patterns of *SHAT1* in the AZ of the *sh4-2* mutant suggests that *SHAT1* might act downstream of, or be positively regulated by, *SH4* during AZ development. To verify this hypothesis, we examined *SH4* expression using in situ hybridization. In the wild type, the convergent expression of *SH4* in the AZ was first visible from early stage sp6 (Figure 7A; see Supplemental Figure 7B online). Notably, *SH4* expression commenced earlier in the AZ than did that of *SHAT1*. Then, *SH4* expression gradually increased in the AZ and anthers during stage sp7 (Figure 7B) and increased further at stage sp8 (Figures 7C and 7D). The *sh4-1* mutation did not change the *SH4* expression pattern, as shown by the expression pattern in *sh4-1* being similar to the wild type (Figures 7E to 7H). By contrast, the *sh4-2* mutation completely disrupted *SH4* expression in AZs (Figures 7I to 7L). These results confirmed that the *sh4-1* allele is different from the *sh4-2*

Figure 3. (continued).

(E) Genotyping of T2 seedlings. H, heterozygous; M, homozygous; W, Huayong.
(F) Comparison of *SHAT1* mRNA expression levels and the nonshattering phenotype in Huayong and 2B70080 mutant. Left: Real-time RT-PCR analysis. Error bars indicate ± SD of the mean of three biological samples. Right: BTS measurement of grain pedicel. Error bars indicate ± SD.
(G) Longitudinal sections across AZs of Huayong and 2B70080 plants. Arrows indicate the AZ. Bars = 50 μm.

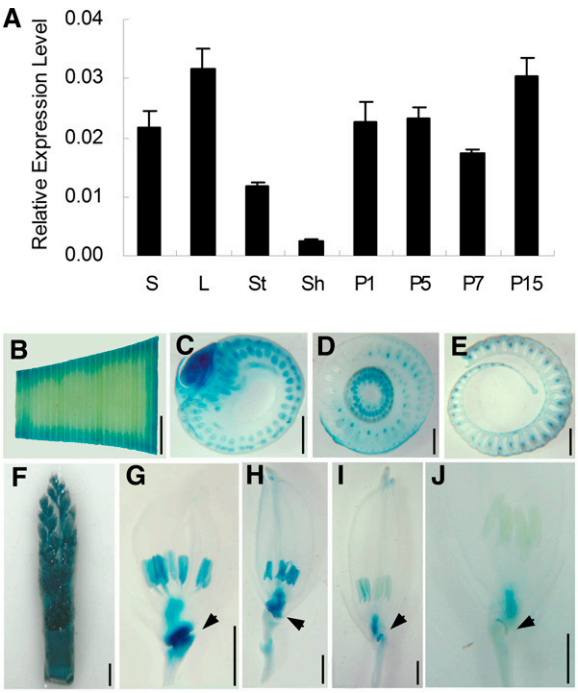

Figure 5. The Expression Pattern of *SHAT1* by Quantitative RT-PCR and GUS Assay.

(A) Quantitative RT-PCR results for *SHAT1* mRNA in different tissues. L, leaf; P1-P15, panicle of 1 to 15 cm lengths, respectively; S, seedling; Sh, sheath; St, stem. Error bars indicate ± SD of the mean of three biological samples.

(B) to **(J)** GUS expression pattern in the $SHAT1_{pro}$:GUS transgenic plant. Leaf **(B)**, stem **(C),** node **(D)**, leaf sheath **(E)**, young panicle **(F)**, and spikelets during different developmental stages **(G)** to **(J)**. Arrows indicate AZ. Bars = 1 mm.

allele. Whereas *sh4-1* still plays a role in specifying AZ identity, *sh4-2* appears to be a null-function mutation. We then determined *SH4* expression in the *shat1* mutant. *SH4* exhibited a nearly intact expression pattern and expression level in the *shat1* mutant until early sp8 stage (Figures 7M to 7O). However, *SH4* transcripts were not detected in most cases from late sp8 stage when *SH4* was expected to concentrate in AZ (Figure 7P). The disappearance of *SH4* expression in the *shat1* mutant suggests that *SHAT1* functions in maintaining *SH4* expression in the AZ during late stage sp8.

The Persistent and Concentrated Expression of *SHAT1* and *SH4* in AZ Is Required for AZ Identification

To explore further the relevance of *SHAT1* and *SH4* to AZ development in rice, we examined the genotypes of *SHAT1* and *SH4* and the AZ phenotype in a number of cultivated varieties. *SH4* is highly conserved in cultivated rice varieties, with almost all varieties possessing the *sh4-1* allele (Zhang et al., 2009). Similarly, *SHAT1* was also conserved in cultivated rice, with few functional variants found in the coding region in genome sequences of 944 rice cultivars (http://www.ncgr.ac.cn/RiceHapMap). However, characterizing the shattering/nonshattering phenotypes showed that some varieties still showed nonshattering and had no AZ, for which the genotypes were *SHAT1* and *sh4-1*. For example, *japonica* cv Nipponbare harbored *SHAT1* and *sh4-1* as did *indica* cv GLA4 (Table 1); however, confocal microscopy and scanning electron microscopy analysis showed that Nipponbare had no AZs (see Supplemental Figures 8A and 8B online).These results suggest the wild-type *SHAT1* and *sh4-1* genotypes do not form AZs.

To explore whether the defect in AZ in Nipponbare was due to the temporal and spatial expression pattern changes of *SHAT1* and *sh4-1*, we performed in situ hybridization of these two genes in Nipponbare. *SHAT1* exhibited obvious signals in the AZ region

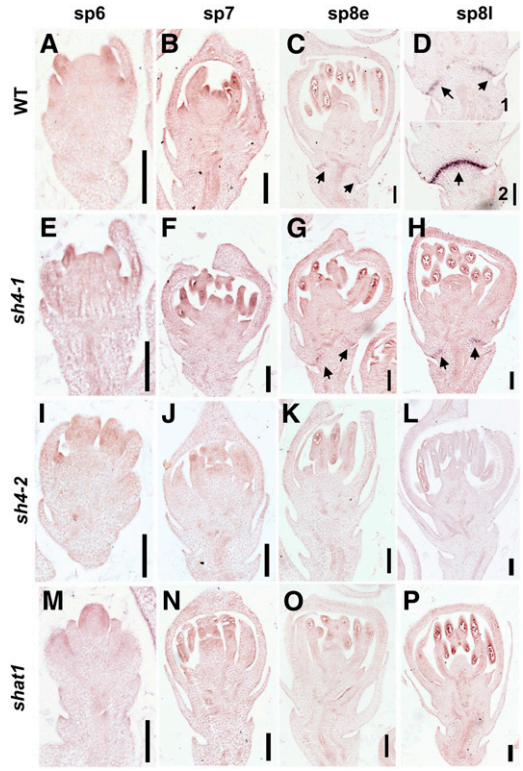

Figure 6. In Situ Hybridization of *SHAT1* during Spikelet Developmental Stages Sp6 to Sp8.

(A) to **(D)** The wild type (WT). *SHAT1* transcripts began to accumulate in the provisional AZ from stage sp8e **(C)** and became intense during stage sp8l **(D)**. Longitudinal sections through vascular bundle (1) or deviate from vascular bundle (2) are shown in **(D)**. Sense probe control is shown in Supplemental Figure 7A online.

(E) to **(H)** *sh4-1* mutant. *SHAT1* exhibited a similar expression pattern to that in the wild type.

(I) to **(L)** *sh4-2* mutant. *SHAT1* expression was completely disrupted in *sh4-2*.

(M) to **(P)** *shat1* mutant. *SHAT1* signals were lost in AZ but retained in anthers **(P)**.

The four columns from left to right indicate spikelet developmental stages sp6 to sp8, respectively. sp8e, early stage sp8; sp8l, late stage sp8. Arrows indicate AZ. Bars = 100 μm.

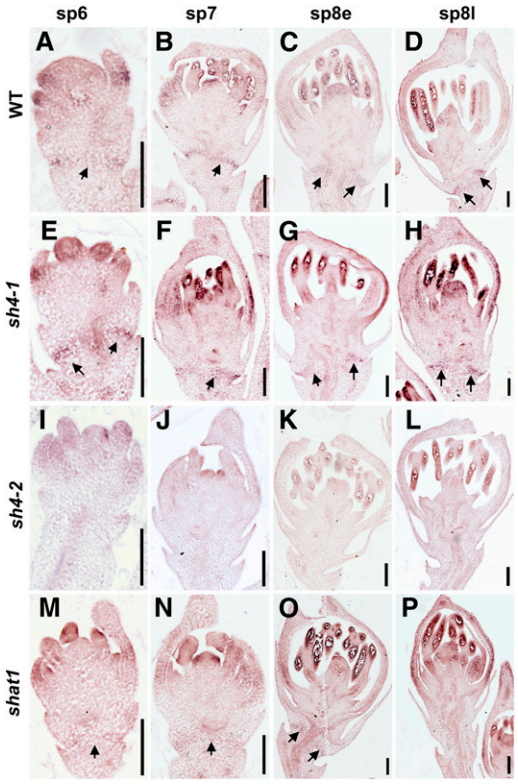

Figure 7. In Situ Hybridization of *SH4* during Spikelet Developmental Stages Sp6 to Sp8.

(A) to **(D)** The wild type (WT). *SH4* transcripts began to accumulate in the provisional AZ from stage sp6 **(A)** and became obvious in AZ and anthers during stage sp7 **(B)**. More intense signals for *SH4* were displayed in early stage sp8 **(C)** and late stage sp8 **(D)**. Sense probe control is shown in Supplemental Figure 7B online.

(E) to **(H)** *sh4-1* mutant. *SH4* exhibited a similar expression pattern to that in the wild type.

(I) to **(L)** *sh4-2* mutant. *SH4* expression was completely disrupted in *sh4-2*.

(M) to **(P)** *shat1* mutant. *SH4* signals were present at AZ during stages sp6-sp8e (**[M]** to **[O]**) but absent from sp8l onward **(P)**.

The four columns from left to right indicate spikelet developmental stages sp6-sp8, respectively. sp8e, early stage sp8; sp8l, late stage sp8. Arrows indicate AZ. Bars = 100 μm.

during early stage sp8, although they were not so convergent compared with that in the wild type (Figures 8A to 8C). However, these signals disappeared from this region during late stage sp8 (Figure 8D). There was a similar situation for *SH4* with nearly intact expression pattern in AZ region from stage sp6 to early stage sp8 (Figures 8E to 8G) but no signals during late stage sp8 (Figure 8H).Therefore, we proposed two questions: Did AZ specification require the continuous expression of active *SHAT1* and *sh4-1* in AZs? Were some functions of a genetic partner in maintaining *SHAT1* and *sh4-1* expression in AZs impaired in Nipponbare? Previous study revealed that *qSH1* was responsible for AZ identification, so the incompetent *qsh1* in Nipponbare may be such a defective genetic partner. To verify our hypothesis, we used a *qSH1* near-isogenic line N52 in which the *qSH1* locus was derived from the *indica* cv 93-11 but the other genetic background was from the *japonica* cv Nipponbare (see Supplemental Figure 9 online). The expression of *qSH1* in N52 exhibited a wild-type like pattern (Figure 9H), in striking contrast with the absent expression in Nipponbare AZs (Konishi et al., 2006). We then determined *SHAT1* and *SH4* expression in N52 and, as expected, expression of both was maintained in AZs during late stage sp8 (Figures 8I to 8L and 8M to 8P) and finally resulted in AZ formation in N52 (see Supplemental Figures 8C and 8D online). These results suggest the identification of a competent AZ requires not only the wild-type *SHAT1* and *sh4-1* genotypes but also their persistent expression in AZ during the AZ differentiation process. *qSH1* had its effect by maintaining *SHAT1* and *SH4* expression in AZ, thus promoting AZ differentiation.

qSH1 Functions Downstream of *SHAT1* and *SH4*

The functions of *qSH1* in maintaining *SHAT1* and *SH4* expression in AZs led us to investigate whether *qSH1* activity was dependent on *SHAT1* and *SH4*. To address this, *qSH1* expression was examined in the wild type and *shat1* and *sh4-2* mutants. In the wild type, the *qSH1* signal commenced in AZ from early stage sp8 (Figures 9A to 9C and 9E). During late stage sp8, the *qSH1* signal became more intense in AZs and anthers (Figure 9D) and closely resembled that of *SHAT1* in the wild type. By contrast, no *qSH1* signal was detected in AZs of either the *shat1* mutant (Figure 9F) or the *sh4-2* mutant (Figure 9G). These results indicated that *qSH1* functions downstream of *SHAT1* and *SH4* in maintaining their expression in the AZ, thus promoting AZ differentiation.

DISCUSSION

SHAT1 Is a Member of the AP2 Family of Genes

The AP2 domain defines a large gene family of mostly plant specific DNA binding proteins called AP2/Ethylene Response Factors (Riechmann and Meyerowitz, 1998). Those carrying two AP2 domain genes are classified into two groups: AP2 and AINTEGUMENTA. The AP2 group members harbor a miR172 target site (Magnani et al., 2004; Kim et al., 2006). Phylogenetic analysis showed that *SHAT1* belongs to the AP2 group and is closely related to barley (*Hordeum vulgare*) *Cleistogamy1* (*Cly1*) and *Arabidopsis AP2* (see Supplemental Figure 10, Supplemental References 1, and Supplemental Data Set 1 online). *Cly1* is known to regulate lodicule development. A synonymous nucleotide substitution at the miR172 targeting site in *Cly1* abolishes miR172-mediated cleavage of *Cly1* and results in the failure to develop normal lodicules, thus producing the cleistogamous phenotype (Nair et al., 2010). In the *shat1* mutant, enlarged and/or an increased number of lodicules was also frequently observed (see Supplemental Figures 2J and 3E online), and, occasionally, lodicules were elongated and transformed into lemma/palea-like organs (see Supplemental Figure 2M online); consequently, these spikelets were unable to close after flowering and resulted in naked grains. These phenotypes were previously observed in transgenic rice plants overexpressing miR172b (Zhu

Table 1. Expression of *SH4*, *SHAT1*, and *qSH1* and the Shattering Phenotypes

Strain	Genotype	Signals at AZs				BTS Value (g)
		Sp6	Sp7	Sp8e	Sp8l	
shat1 sh4-2	*shat1*	−	−	−	−	101 ± 8.7 (Nonshattering)
	sh4-2	−	−	−	−	
	qSH1	−	−	−	−	
sh4-2	*SHAT1*	−	−	−	−	105 ± 6.5 (Nonshattering)
	sh4-2	−	−	−	−	
	qSH1	−	−	−	−	
shat1	*shat1*	−	−	−	−	100 ± 9.5 (Nonshattering)
	SH4	+	+	+	−	
	qSH1	−	−	−	−	
Nipponbare	*SHAT1*	−	−	+	−	109 ± 4.0 (Nonshattering)
	sh4-1	+	+	+	−	
	qsh1	−	−	−	−	
N52	*SHAT1*	−	−	+	++	37 ± 5.3 (Reduced shattering)
	sh4-1	+	+	+	+	
	qSH1	−	−	+	+	
GLA4	*SHAT1*	−	−	+	++	29 ± 1.7 (Reduced shattering)
	sh4-1	+	+	+	+	
	qSH1	−	−	+	+	
Wild type	*SHAT1*	−	−	+	++	0 (Easy shattering)
	SH4	+	+	+	+	
	qSH1	−	−	+	+	

The plant materials and their genotypes for the three genes are indicated. The expression signals of the three genes detected using in situ hybridization during different spikelet developmental stages are shown. The corresponding BST values were measured when the seeds were fully ripened and are indicated by average ± SD. Sp8e, early stage sp8; Sp8l, late stage sp8; −, no signal; +, intermediate signal; ++, strong signal.

et al., 2009). These results suggest that miR172-mediated cleavage of *SHAT1* might also be essential for normal flower opening in rice. However, the seed shattering defects we observed in the rice *shat1* mutant were not reported in the barley *cly1* mutant (Nair et al., 2010). Similarly, *AP2* in *Arabidopsis* has been shown to influence many critical aspects of development, from regulating reproductive organ morphogenesis (Jofuku et al., 2005; Ohto et al., 2005; Würschum et al., 2006; Yant et al., 2010) to determining flowering time (Yant et al., 2010); however, none of them are related to cell separation processes, such as petal abscission or fruit dehiscence.

As far as we know, the sole *AP2* gene reported to affect seed shattering is the wheat *Q* gene; this affects a repertoire of characters important for domestication, such as threshability, glume shape, and glume tenacity (Simons et al., 2006). Although *Q* may represent a duplicate paralog distinct from rice *SHAT1*, the defects of the AZ phenotype in *q* greatly resembled those of *shat1*. A single spikelet of wheat is composed of three fertile florets and a pair of glumes. The AZ is close to the base of the glumes. The mutant *q* spikelet also has three fertile florets and a pair of glumes, but the region destined to be the AZ is substituted by a longer rachilla (Simons et al., 2006). The rice spikelet is similar to that of wheat; however, in rice, the second and third florets degenerate into sterile lemmas and the original glumes degenerate into rudimentary glumes (Yoshida and Nagato, 2011). The AZ is located between the sterile lemmas and the rudimentary glumes. In the *shat1* mutant, the region destined to be the AZ was substituted by a longer and crook-neck-like rachilla. The comparable AZ phenotype caused by the paralog *shat1* and *q* genes suggests that rice and wheat may share similar mechanisms in seed AZ development.

SHAT1 Expression and AZ Differentiation

A previous anatomical study of AZs in rice revealed that the AZ could be observed by elongation of cells in the pedicel and rachilla when the panicle length was 20 to 30 mm and spikelet length was around 2 mm (Jin, 1986). Studies on oat (*Avena sativa*), another monocotyledon, also showed that prior to cell separation the site where cell wall breakdown will take place was well defined (Hoekstra et al., 2001). In this study, *SHAT1* mRNA accumulated in AZs as early as sp8 stage when carpel primordia began to differentiate. However, we cannot rule out whether the morphological differentiation process of AZ cells starts at sp8 stage, since provisional AZ cells generally appear very similar to adjacent cells during this period. Our observations showed that the time when AZ cells were first distinguishable from adjacent cells in the wild type was around 15 d before heading (see Supplemental Figures 11A and 11D online). During this time, the length of spikelet was around 2 to 3 mm, whereas in contemporaneous *shat1* mutant, such one or two layers of flattened and small AZ cells were not observed (see Supplemental Figures 11B and 11C online). Another interesting finding was that the expression intensity of *SHAT1* increased with development of the spikelet (Figures 6C and 6D). One possible explanation is that *SHAT1* may be positively regulated by its gene products. *Arabidopsis AP2* was reported to participate in a self-feedback loop

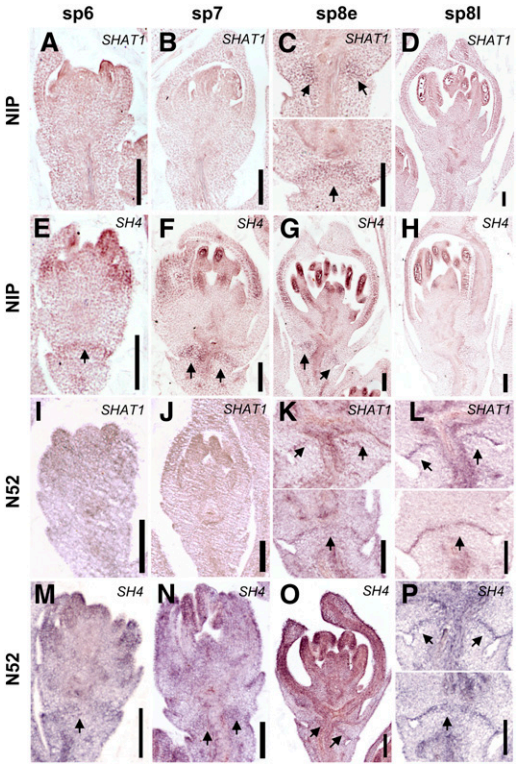

Figure 8. Effect of Persistent and Concentrated Expression of *SHAT1* and *SH4* on AZ Differentiation.

(A) to **(D)** Expression of *SHAT1* in *japonica* cv Nipponbare. *SHAT1* expression gathered in AZ during stage sp8e **(C)** but absent from the AZ during stage sp8l **(D)**.
(E) to **(H)** Expression of *SH4* in *japonica* cv Nipponbare. *SH4* expression emerged in AZ from stage sp6 **(E)** and remained in the AZ from stage sp7 **(F)** to stage sp8e **(G)** but disappeared from the AZ during stage sp8l **(H)**.
(I) to **(L)** Expression of *SHAT1* in substitution line N52. *SHAT1* expression persisted in the AZ from stage sp8e **(K)** to sp8l **(L)**.
(M) to **(P)** Expression of *SH4* in substitution line N52. *SH4* transcripts accumulated in the AZ during stages sp6-sp8l.
The four columns from left to right indicate spikelet developmental stages sp6-sp8, respectively. sp8e, early stage sp8; sp8l, late stage sp8. Arrows indicate AZ. Bars = 100 μm.

through negatively regulating its inhibitor miR172 (Yant et al., 2010), and a similar mechanism may exist in rice.

New Insight into *SH4* Function in AZ Specification

SH4 has previously been identified to affect AZ formation as well as the hydrolysis process (Li et al., 2006). Here, we identified a new *SH4* allelic mutation, *sh4-2*. Confocal microscopy and scanning electron microscopy analysis showed that phenotypes of the AZ in *sh4-2* were very different from that resulting from the cultivated rice *sh4-1* allele. Compared with the isodiametrically flattened and thin-walled appearance in *sh4-1*, AZ cells in *sh4-2* had a flattened shape but lost the thin-walled property (Figure 1R; see Supplemental Figure 5A online). Moreover, in situ hybridization results showed that the expression of *SH4* in the *sh4-2* mutant was completely abolished (Figure 7L), whereas it showed a wild-type-like pattern in *sh4-1* (Figure 7H). Therefore, *sh4-2* was assumed to be a null-function mutant. However, one of the most unexpected findings in this study was that the *sh4-2* mutation suppressed the *sh4-1* phenotype. Plants with these intragenic suppressor mutations had a similar seed-shattering habit to wild-type plants (see Supplemental Figure 12 online). This originally led us to the conclusion that *sh4-2* could be a different locus from the cultivated rice *sh4-1*. Since *sh4-2* had a one-nucleotide insertion in the second exon of *SH4*, whereas *sh4-1* had a one-nucleotide substitution in the first exon, the functional SH4 may be a hybrid multimeric protein formed from different domains produced by different mutant alleles. This hypothesis is supported by the finding that SH4 protein is predicted to have a coiled-coil structure that probably forms a homopolymer. Examples of intragenic complementation through forming a tetrameric protein include *ASL* in human (Turner et al., 1997). However, in situ hybridization did not detect *SH4* expression in the *sh4-2* mutant, leading to the question of how a heterodimer could be generated if the *sh4-2* allele lacked any mRNA. Since the in situ technique could not quantify the gene expression levels, we performed quantitative RT-PCR to detect any expression of *SH4* in *sh4-1* and *sh4-2* mutants (see Supplemental Figure 13A online). Compared with the wild type, *SH4* showed a decrease in both *sh4-1* and *sh4-2*, with a greater decline in *sh4-2*. The presence of some expression of *SH4* in *sh4-2* seems inconsistent with the in situ results, although this may reflect the higher resolution of the quantitative RT-PCR technique.

Dissecting the Relative Contribution of *SHAT1, SH4,* and *qSH1* to Seed AZ Differentiation

SHAT1, *SH4*, and *qSH1* are three important genes involved in AZ differentiation. We summarized the relationship between their

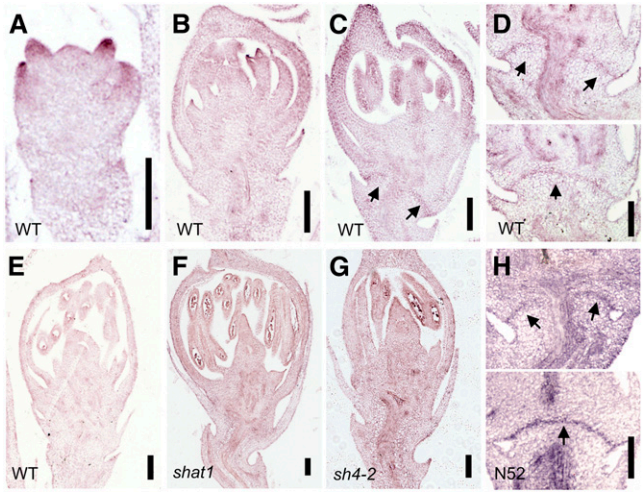

Figure 9. In Situ Hybridization of *qSH1*.

(A) to **(E)** Expression of *qSH1* in wild type (WT) during stages sp6-sp8l. Sense probe as control in **(E)**.
(F) to **(H)** Stage sp8l in different spikelets. No signals for *qSH1* were detected in the *shat1* spikelet **(F)** or in the *sh4-2* spikelet **(G)**; strong signals for *qSH1* were detected in N52 AZs **(H)**. sp8e, early stage sp8; sp8l, late stage sp8. Arrows indicate AZ. Bars = 100 μm.

expression and shattering phenotype in Table 1. *SH4* seemed to play a role early in AZ formation. The earliest accumulation of *SH4* in AZ and the inability to detect *SHAT1* and *qSH1* expression in AZs of the *sh4-2* mutant suggest that *SH4* acts largely upstream of *SHAT1* and *qSH1* (Figure 10). The highly accumulated *SH4* may confer the provisional AZ cells with some properties that distinguish them from their neighbors, thus providing clues for *SHAT1* and *qSH1* accumulation in a narrow strip of AZ cells. The in situ hybridization results showed that only after *SH4* accumulated in the AZ did *SHAT1* and *qSH1* expression begin to be limited to the AZ, then becoming more intense in the AZ with the development of spikelet (Table 1). Our results provide a striking contrast to previous reports that *qSH1* had a stronger effect on seed shattering than did *sh4-1* in the genetic background of *japonica* cv Nipponbare (Onishi et al., 2007; Ishikawa et al., 2010). We interpret this discrepancy as suggestive of different effects from the different mutation alleles of *SH4*. Since the *sh4-1* allele in cultivated rice was still functional, it is difficult to decipher the genetic interaction among *SH4* and other shattering-related genes. By contrast, *sh4-2* is a presumed null-function mutation, which afforded us a good opportunity to explore the function of *SH4* in the shattering pathway.

SHAT1 appeared to play a dual-functional role in AZ specification: functioning downstream of *SH4* to activate *qSH1* expression and maintaining the expression of *SH4* in the AZ (Figure 10). The inability to detect *qSH1* expression in the *shat1* mutant suggests that *qSH1* is activated by *SHAT1* rather than by *SH4*, given that *SH4* still exhibited intact expression in *shat1* during early stage sp8, when *qSH1* was expected to be expressed in the AZ (Table 1). However, we cannot rule out that this activation could be fulfilled by *SHAT1* alone or may require the help of *SH4*. More experiments should be performed to examine *qSH1* expression in the *sh4-2* background and how *SHAT1* expression was maintained in AZ. On the other hand, the disappearance of *SH4* expression in the *shat1* AZ during late-stage sp8 suggests that *SHAT1* plays an important role in maintaining *SH4* expression in the AZ, which is required for AZ identity (Table 1). The *SHAT1*-dependent activity of *SH4* was much more apparent when comparing AZ phenotypes of *shat1*, *sh4-2*, and *shat1 sh4-2* mutants. The AZ phenotype of *shat1 sh4-2* was similar to that of *shat1*, which developed a crook-neck-like rachilla (Figure 1V) and showed peanut-like cortical cells in the AZ position (Figures 1W and 1X). This is compatible with the result that *shat1 sh4-2* showed

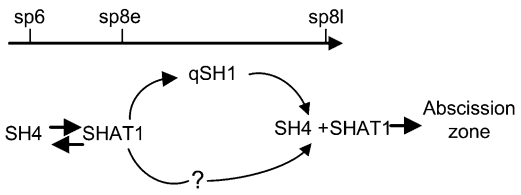

Figure 10. A Genetic Model of Regulatory Network Specifying AZ Development in Rice.

The continuous expression of *SHAT1* and *SH4*, regulated by *qSH1* or other genetic partners (as shown by the question mark), is necessary for proper AZ development. Long horizontal arrow represents time progression. sp8e, early stage sp8; sp8l, late stage sp8.

similar changes in BTS values to *shat1* rather than to *sh4-2* (Figure 1B). Although both *shat1* and *sh4-2* did not develop AZs, we observed different changes in BTS values among these two mutant lines, with *sh4-2* showing higher values before 13 d (Figure 1B). We explain these results as the crook-neck-like structure being able to endure only around 150-g pull-off forces without fracturing. Therefore, the BTS values of *shat1* and *shat1 sh4-2* were even lower than for the wild type before 9 d (Figure 1B).

In addition to these two functions, *SHAT1* seemed to play other roles independent of *SH4*. This hypothesis is supported by two findings: First, there were various spikelet defects seen in the *shat1* mutant but not the *sh4-2* mutant (see Supplemental Figures 2B to 2E online); second, *SHAT1* maintained some expression in the *sh4-2* mutant. Although we did not detect *SHAT1* expression in the *sh4-2* mutant using in situ hybridization, *SHAT1* showed a slight increase in *sh4-1* and a modest repression in the *sh4-2* mutant (see Supplemental Figure 13B online) using quantitative RT-PCR. The reduced, yet persistent, expression of *SHAT1* in the *sh4-2* mutant suggests that *SHAT1* expression is not simply regulated by *SH4*. The *sh4-2* mutation disrupted *SHAT1* expression in AZs, whereas the other expression domains, such as anthers, might be unaffected.

qSH1 affects the maintenance of *SHAT1* and *SH4* expression in the AZ, thus promoting the AZ differentiation process (Figure 10). In *japonica* cv Nipponbare, the expression of *SHAT1* and *SH4* receded from the AZ during late stage sp8 and ultimately the AZ was not formed (Table 1). Conversely, the defective AZ phenotype in Nipponbare was suppressed by sustained expression of *SHAT1* and *SH4* in the AZ after introgression of a functional *qSH1* locus from *indica* cv 93-11. These results suggest that *qSH1* functions in maintaining *SHAT1* and *SH4* expression in the AZ, thus promoting AZ identity specification. However, *qSH1* may not be the only genetic partner determining the expression of *SHAT1* and *SH4* in the AZ, as some *qSH1*-defective rice subspecies appeared to show a reduced-shattering habit (Konishi et al., 2006). Since we are not sure whether AZs are present in these rice subspecies and how the *qSH1* behaves in them, more experiments should be performed to test the possibility if one or more factor(s) (in addition to *qSH1*) are able to sustain the expression of *SH4* and *SHAT1* in AZs, thus promoting AZ differentiation.

Selection for Shattering Genes in Domestication

Selection of reduced seed shattering is still an important challenge in many agricultural crops worldwide (Gan et al., 2008). In the process of rice domestication, artificial selection is likely to have favored mutation that reduced but did not completely eliminate grain shattering. The cultivated rice *sh4-1* allele achieved an ideal balance between shattering and threshing during rice domestication. Zhang et al. (2009) demonstrated that this reduced-shattering *sh4-1* allele was quickly fixed in all rice cultivars, with levels of sequence polymorphism significantly reduced in both *indica* and *japonica* cultivars relative to the wild progenitors. To explore whether mutations in the *SHAT1* gene also occur in the natural population, we determined the polymorphism of *SHAT1* in different rice landraces. Our high-throughput sequencing results (http://www.ncgr.ac.cn/RiceHapMap) of 614 accessions of landraces from China and 330 accessions of international varieties showed 19 SNPs located in the

SHAT1 genic region (Huang et al., 2010): Eight were located in the UTR regions, four in introns, and seven in exons. Those SNPs generated few functional variants, with most cultivated varieties having the same protein sequence as that in *O. rufipogon* W1943. Therefore, differing from *SH4*, *SHAT1* might not be subject to artificial selection during domestication.

METHODS

Mutant Material and Growth Conditions

Firstly, we constructed a CSSL designated as SL4 in the *Oryza sativa* ssp *indica* cv GLA4 background with the whole chromosome 4 substituted by *Oryza rufipogon* W1943 with the average density of detecting markers of ~2.5 Mb (see Supplemental Figures 1A and 1B online). We then treated ~10,000 T0 generation seeds of SL4 with ^{60}Co γ-rays (65 Gy) and generated 4800 lines in the T1 generation. We screened for nonshattering mutants in the T1 generation. The mutant line 2B70080 was identified in the T-DNA insertion line database (Jeon et al., 2000). The *indica* cv GLA4 and the *japonica* cv Nipponbare were used as *sh4-1* mutant line and *qsh1* mutant line, respectively, according to the previous sequencing results (Konishi et al., 2006; Li et al., 2006). All plants (*O. sativa*) were grown in the paddy field of Shanghai Plant Physiology and Ecology, Shanghai, China.

Characterization of Mutant Phenotype

Plants materials were photographed with a Nikon E5400 digital camera and a Nikon SMZ1000 dissecting microscope. For scanning electron microscopy observation, the spikelets of SL4 and *shat1* at ~35 d after heading were collected and processed essentially as described by Keijzer et al. (1996) and observed with a JSM-6360LV scanning electron microscope (Jeol). Confocal microcopy was performed as described by Li et al. (2006). For shattering degree tests, the BTS upon detachment of seeds from the pedicels by pulling was measured by a digital force gauge (Qin et al., 2010). For an individual plant, a total of 100 flowers or grains from five panicles were measured. For transgenic plants, measurement was made on panicles ~30 d after anthesis.

Cloning of *SHAT1* and *SHAT2*

For the positional cloning of *SHAT1*, *shat1* was crossed with *O. sativa* ssp *japonica* cv Nipponbare. A total of 300 crook-neck-like F2 plants were selected for mapping analysis. DNA was extracted from fresh leaves according to the cetyl-trimethylammonium bromide method (Murray and Thompson., 1980) with minor modifications. The molecular markers used in this study are listed in Supplemental Table 1 online. Mutation sites in *shat1* were determined by PCR amplification and sequencing analysis.

For the positional cloning of *SHAT2*, *shat2* was first crossed with *japonica* cv Nipponbare. A total of 96 F2 plants that exhibited a nonshattering phenotype and had *SH4* and *qSH1* loci from *shat2* were selected for primary mapping analysis. After *SHAT2* was mapped to the long arm of chromosome 4, *shat2* was then crossed with *indica* cv GLA4 to construct a new F2 population. There were 907 nonshattering F2 plants selected for fine mapping.

RNAi Experiment

To generate the *SHAT1*-RNAi construct for *SHAT1* gene suppression, a 426-bp fragment of *SHAT1* cDNA was PCR amplified with primer *SHAT1*-RNAi-F (5′-cggggtaccactagtCAACCGCTACAGCAGCTGCA-3′, *Kpn*I, *Spe*I) and *SHAT1*-RNAi-R (5′-cgcggatccgagctcACTGCTTGAGGCGACGCTTG-3′, *Bam*HI, *Sac*I), which harbors restriction sites (set in lowercase letters) for cloning. The resulting PCR products were first digested by *Spe*I and *Sac*I and ligated into vector pTCK303 (Wang et al., 2004) to get the transitional vector. Then, the PCR products were digested by *Kpn*I and *Bam*HI and ligated into the transitional vector. The resulting RNAi construct was used for knockdown of gene expression.

RNA Extraction and Quantitative RT-PCR Analysis

Total RNA was extracted using the Trizol reagent (Invitrogen) according to the manufacturer's instructions. After treatment with DNaseI (NEB), 5 μg of total RNA was used to synthesize the oligo(dT) primed first-strand cDNA using SuperScript II reverse transcriptase (Invitrogen). Quantitative RT-PCR was performed on the Applied Biosystems 7500 real-time PCR System. Diluted cDNA was amplified using SYBR Premix Ex Taq (TaKaRa). The levels of *SHAT1* transcripts were normalized by endogenous *Ubiquitin* transcripts. Each set of experiments was repeated three times. Primers used for quantitative real-time PCR are listed in Supplemental Table 2 online.

Nuclear Localization Analysis and Transactivation Assay

To construct the SHAT1-GFP fusion plasmid, the full-length *SHAT1* coding region without stop codon was PCR amplified with primers containing *Xho*I and *Spe*I site (see Supplemental Table 2 online) and was then in-frame cloned into the *Xho*I-*Spe*I site of pA7 (Peng et al., 2008), which contained a GFP coding sequence under the control of 35S promoter (kindly provided by Zhang Jingliu). Transient expression of the pA7- SHAT1-GFP fusion in onion epidermal cells was performed as previously described (Scott et al., 1999) using a helium biolistic device (PDS-1000; Bio-Rad). The samples were observed with a confocal laser microscope (LSM510; Zeiss).

We performed the transactivation activity assay using the yeast one-hybrid system (Clontech). To construct pGBKT7-SHAT1, pGBKT7-SHAT1ΔC (1 to 326), and pGBKT7-SHAT1ΔN (112 to 459), the full-length coding sequence and the N and C termini of SHAT1 were amplified by PCR (see Supplemental Table 2 online). The PCR products were digested with *Eco*RI and *Bam*HI and cloned into pGBKT7 to fuse to the GAL4 binding domain. We transformed all vectors into yeast strain AH109 using electroporation and selected on SD/Trp- plates. After 2 d of incubation at 30°C, the yeast colonies were diluted to an OD_{600} of 0.5 and dropped on either SD/Trp-/Ade- plates or SD/Trp-/His- plates with 0.5 mM of 3AT. These plates were incubated at 30°C until yeast cells grew to form colonies.

Construction of the *SHAT1* Promoter-GUS Fusion and GUS Assay

For constructing the *SHAT1* promoter:GUS fusion plasmid, a 2.3-kb region (from −2393 to −66 bp from the translation start site) was PCR amplified from *japonica* cv Nipponbare with primers containing *Sal*I and *Bam*HI (see Supplemental Table 2 online). After digestion, the released segment was ligated upstream of the GUS in the pCAMBIA1300GN:GUS (Ren et al., 2005) (kindly provided by Lin Hongxuan).

For detection of GUS activity, tissue was fixed in 90% acetone for 1 h at 4°C and then rinsed with GUS buffer (100 mM NaH_2PO_4/Na_2HPO_4, pH 7.0, 10 mM EDTA, 0.1% Triton X-100, 0.5 mM potassium ferricyanide, and 0.5 mM potassium ferrocyanide). Samples were incubated with GUS buffer supplemented with 0.05% 5-bromo-4- chloro-3-indolyl β-D-glucuronide cyclohexylamine salt (Rose Scientific) at 37°C overnight. Then, tissues were cleared overnight in destaining buffer (ethanol: acetic acid = 84:16) and washed several times with 70% ethanol before observation under a dissecting microscope.

In Situ Hybridization

Young panicles were fixed in 4% paraformaldehyde, dehydrated through an ethanol series, embedded in paraplast (Sigma-Aldrich), and sectioned at 8-μm thickness using a rotary microtome (Leica). A 426-bp gene-specific

region of *SHAT1* cDNA, amplified by PCR reaction (primers 5′-CAACCGCTACAGCAGCTGCA-3′ and 5′-ACTGCTTGAGGCGACGCTTG-3′); a 446-bp gene-specific region of *SH4* cDNA, amplified by PCR reaction (primers 5′-ATCATCGGCCGGAGGAGTCG-3′ and 5′-GCACCACCATCACGGCCATC-3′); and a 227-bp gene-specific region of *qSH1* cDNA, amplified by PCR reaction (primers 5′-CGAAGCTCATCTCCATGATG-3′ and 5′-TGCAGGAAGTGTTCGAACAG-3′), were used as the probes. The amplified DNA fragments were subcloned into a pGEM-T easy vector (Promega) in two orientations; the sense and antisense probes were synthesized and used to generate the RNA probe. In situ hybridization was performed as described (Luo et al., 1996).

Accession Numbers

Sequence data from this article can be found in the GenBank/EMBL data libraries under the following accession numbers: *SHAT1* (FO082280), *SH4* (EF203243), *sh4-1* (LOC_Os04g57530), *qSH1* (LOC_Os01g62920), *AP2* (At4g36920), *LIPLESS2* (AY223519), *Cly1* (GQ403050), *IDS1* (GI63937834), *Q* (AY702960), *SNB* (LOC_Os07g13170), and *GLOSSY15* (AY714877). Accession numbers for the sequences used in the phylogenetic analysis are on the tree in Supplemental Figure 10 and Supplemental References 1 online.

Supplemental Data

The following materials are available in the online version of this article.

Supplemental Figure 1. Construction of Chromosome 4 Segment Substitution Line in the GLA4 Background.

Supplemental Figure 2. Phenotype Comparison of the Wild Type, *shat1* Mutant, *shat2* Mutant, and *shat1 shat2* Mutant.

Supplemental Figure 3. Phenotypic Characterization of Panicle Traits and Floral Organ Numbers in the Wild Type and *shat1* Mutant.

Supplemental Figure 4. Grain Size Comparison of the Wild Type and *shat2* Mutant.

Supplemental Figure 5. Morphological Characteristics of AZ in GLA4.

Supplemental Figure 6. Subcellular Localization of SHAT1.

Supplemental Figure 7. The Sense Probe Control of *SHAT1* and *SH4* in the Wild Type during Late-Stage Sp8.

Supplemental Figure 8. Longitudinal Sections and Scanning Electron Microscopy Photos of Nipponbare and N52.

Supplemental Figure 9. The Genotype of the Chromosome Segment Substitution Line N52.

Supplemental Figure 10. Phylogenetic Tree of the AP2 Subgroup Genes Containing Two AP2 Domains and MiR172 Target Site from Rice and Other Species.

Supplemental Figure 11. Anatomical Structure of the AZ in the Wild Type and *shat1* Mutant during Early Spikelet Development Stage.

Supplemental Figure 12. Shattering Phenotype Comparison of *sh4-1* Mutant, *sh4-2* Mutant, and F1 Plant of *sh4-1/sh4-2*.

Supplemental Figure 13. Quantitative RT-PCR Results for *SHAT1* and *SH4* mRNA in Wild-Type and Mutant Lines.

Supplemental Table 1. The Molecular Marker Primers Used in Map-Based Cloning.

Supplemental Table 2. The Primers Used for Plasmid Construction and Functional Analysis.

Supplemental Data Set 1. Alignment of AP2 Subgroup Genes Used for the Phylogenetic Analysis Shown in Supplemental Figure 10.

Supplemental References 1. Supplemental References for Supplemental Figure 10.

ACKNOWLEDGMENTS

We thank Hongquan Yang (Shanghai Jiao Tong University) and Zhenbiao Yang (University of California, Riverside) for critical reading of the manuscript. We thank Jiqin Li for resin sections, Zhiping Zhang for scanning electron microscopy observation, and Hongxuan Lin for providing the vector pCAMBIA1300GN at the Institute of Plant Physiology and Ecology, Chinese Academy of Sciences. We thank Kang Chong for providing the vector pTCK 303 at the Institute of Botany, Chinese Academy of Sciences. We thank Qiaoquan Liu for providing us the CSSL line N52 (Yangzhou University), and Gynheung An for providing the T-DNA insertion mutant line 2B70080 (Kyung Hee University). This work was supported by the Ministry of Science and Technology of China (2011CB100205, 2012AA10A302 and 2012AA10A304), and the Ministry of Agriculture of China (2011ZX08001-004 and 2011ZX08009-002), the National Natural Science Foundation of China (31121063), and the Chinese Academy of Sciences to B.H.

AUTHOR CONTRIBUTIONS

Y.Z., D.L., B.Z., and B.H. designed the experiment. Y.Z., D.L., C.L., J.L., B.Z., B.-F.Z., Z.W., Y.S., and J.Z. performed the experiment and analyzed the data. T.S. supervised measuring pedicel BTS and gene cloning. Y.Z. and B.H. wrote the article.

Received December 2, 2011; revised February 12, 2012; accepted February 22, 2012; published March 9, 2012.

REFERENCES

Briggs, C.L., and Morris, E.C. (2008). Seed-coat dormancy in *Grevillea linearifolia*: Little change in permeability to an apoplastic tracer after treatment with smoke and heat. Ann. Bot. (Lond.) **101:** 623–632.

Chen, X.M. (2004). A microRNA as a translational repressor of APETALA2 in *Arabidopsis* flower development. Science **303:** 2022–2025.

Doebley, J. (2006). Plant science. Unfallen grains: How ancient farmers turned weeds into crops. Science **312:** 1318–1319.

Fuller, D.Q., Qin, L., Zheng, Y.F., Zhao, Z.J., Chen, X., Hosoya, L.A., and Sun, G.P. (2009). The domestication process and domestication rate in rice: spikelet bases from the Lower Yangtze. Science **323:** 1607–1610.

Gan, Y., Malhi, S.S., Brandt, S.A., and McDonald, C.L. (2008). Assessment of seed shattering resistance and yield loss in five oilseed crops. Can. J. Plant Sci. **88:** 267–270.

Hoekstra, G.J., Darbyshire, S.J., and Mather, D.E. (2001). Anatomical features at the disarticulation zone in florets of fatuoid and nonfatuoid oat (*Avena sativa* L.). Can. J. Bot. **79:** 1409–1416.

Huang, X.H., et al. (2010). Genome-wide association studies of 14 agronomic traits in rice landraces. Nat. Genet. **42:** 961–967.

Ishikawa, R., Thanh, P.T., Nimura, N., Htun, T.M., Yamasaki, M., and Ishii, T. (2010). Allelic interaction at seed-shattering loci in the genetic backgrounds of wild and cultivated rice species. Genes Genet. Syst. **85:** 265–271.

Itoh, J., Nonomura, K., Ikeda, K., Yamaki, S., Inukai, Y., Yamagishi, H., Kitano, H., and Nagato, Y. (2005). Rice plant development: from zygote to spikelet. Plant Cell Physiol. **46:** 23–47.

Jeon, J.S., et al. (2000). T-DNA insertional mutagenesis for functional genomics in rice. Plant J. **22:** 561–570.

Ji, H., et al. (2010). Inactivation of the CTD phosphatase-like gene OsCPL1 enhances the development of the abscission layer and seed shattering in rice. Plant J. **61:** 96–106.

Jin, I.D. (1986). On the formation and development of abscission layer in rice plants, *Oryza sativa*. Jpn. J. Crop. Sci. **55:** 451–457.

Jofuku, K.D., Omidyar, P.K., Gee, Z., and Okamuro, J.K. (2005). Control of seed mass and seed yield by the floral homeotic gene APETALA2. Proc. Natl. Acad. Sci. USA **102:** 3117–3122.

Keijzer, C.J., Reinders, M.C., and LeferinkTenKlooster, H.B. (1996). The mechanics of the grass flower: The extension of the staminal filaments and the lodicules of maize. Ann. Bot. (Lond.) **77:** 675–683.

Kim, S., Soltis, P.S., Wall, K., and Soltis, D.E. (2006). Phylogeny and domain evolution in the APETALA2-like gene family. Mol. Biol. Evol. **23:** 107–120.

Konishi, S., Izawa, T., Lin, S.Y., Ebana, K., Fukuta, Y., Sasaki, T., and Yano, M. (2006). An SNP caused loss of seed shattering during rice domestication. Science **312:** 1392–1396.

Li, C.B., Zhou, A.L., and Sang, T. (2006). Rice domestication by reducing shattering. Science **311:** 1936–1939.

Lin, Z., Griffith, M.E., Li, X., Zhu, Z., Tan, L., Fu, Y., Zhang, W., Wang, X., Xie, D., and Sun, C. (2007). Origin of seed shattering in rice (*Oryza sativa* L.). Planta **226:** 11–20.

Lu, G., Gao, C.X., Zheng, X.N., and Han, B. (2009). Identification of OsbZIP72 as a positive regulator of ABA response and drought tolerance in rice. Planta **229:** 605–615.

Luo, D., Carpenter, R., Vincent, C., Copsey, L., and Coen, E. (1996). Origin of floral asymmetry in Antirrhinum. Nature **383:** 794–799.

Magnani, E., Sjölander, K., and Hake, S. (2004). From endonucleases to transcription factors: evolution of the AP2 DNA binding domain in plants. Plant Cell **16:** 2265–2277.

McKim, S.M., Stenvik, G.E., Butenko, M.A., Kristiansen, W., Cho, S.K., Hepworth, S.R., Aalen, R.B., and Haughn, G.W. (2008). The BLADE-ON-PETIOLE genes are essential for abscission zone formation in *Arabidopsis*. Development **135:** 1537–1546.

Murray, M.G., and Thompson, W.F. (1980). Rapid isolation of high molecular weight plant DNA. Nucleic Acids Res. **8:** 4321–4325.

Nair, S.K., et al. (2010). Cleistogamous flowering in barley arises from the suppression of microRNA-guided HvAP2 mRNA cleavage. Proc. Natl. Acad. Sci. USA **107:** 490–495.

Ohto, M.A., Fischer, R.L., Goldberg, R.B., Nakamura, K., and Harada, J.J. (2005). Control of seed mass by APETALA2. Proc. Natl. Acad. Sci. USA **102:** 3123–3128.

Onishi, K., Takagi, K., Kontani, M., Tanaka, T., and Sano, Y. (2007). Different patterns of genealogical relationships found in the two major QTLs causing reduction of seed shattering during rice domestication. Genome **50:** 757–766.

Peng, L.T., Shi, Z.Y., Li, L., Shen, G.Z., and Zhang, J.L. (2008). Overexpression of transcription factor OsLFL1 delays flowering time in *Oryza sativa*. J. Plant Physiol. **165:** 876–885.

Qin, Y., Kim, S.M., Zhao, X.H., Jia, B.Y., Lee, H.S., Kim, K.M., Eun, M.Y., Jin, I.D., and Sohn, J.K. (2010). Identification for quantitative trait loci controlling grain shattering in rice. Genes Genomics. **32:** 173–180.

Ren, Z.H., Gao, J.P., Li, L.G., Cai, X.L., Huang, W., Chao, D.Y., Zhu, M.Z., Wang, Z.Y., Luan, S., and Lin, H.X. (2005). A rice quantitative trait locus for salt tolerance encodes a sodium transporter. Nat. Genet. **37:** 1141–1146.

Riechmann, J.L., and Meyerowitz, E.M. (1998). The AP2/EREBP family of plant transcription factors. Biol. Chem. **379:** 633–646.

Scott, A., Wyatt, S., Tsou, P.L., Robertson, D., and Allen, N.S. (1999). Model system for plant cell biology: GFP imaging in living onion epidermal cells. Biotechniques **26:** 1125–1132.

Simons, K.J., Fellers, J.P., Trick, H.N., Zhang, Z.C., Tai, Y.S., Gill, B.S., and Faris, J.D. (2006). Molecular characterization of the major wheat domestication gene Q. Genetics **172:** 547–555.

Szymkowiak, E.J., and Irish, E.E. (1999). Interactions between jointless and wild-type tomato tissues during development of the pedicel abscission zone and the inflorescence meristem. Plant Cell **11:** 159–175.

Taghizadeh, M.S., Crawford, S., Nicolas, M.E., and Cousens, R.D. (2009). Water deficit changes the anatomy of the fruit abscission zone in *Raphanus raphanistrum* (*Brassicaceae*). Aust. J. Bot. **57:** 708–714.

Taylor, J.E., and Whitelaw, C.A. (2001). Signals in abscission. New Phytol. **151:** 323–339.

Turner, M.A., Simpson, A., McInnes, R.R., and Howell, P.L. (1997). Human argininosuccinate lyase: A structural basis for intragenic complementation. Proc. Natl. Acad. Sci. USA **94:** 9063–9068.

Wang, M., Chen, C., Xu, Y.Y., Jiang, R.X., Han, Y., Xu, Z.H., and Chong, K. (2004). A practical vector for efficient knockdown of gene expression in rice (*Oryza sativa* L.). Plant Mol. Biol. Rep. **22:** 409–417.

Wollmann, H., Mica, E., Todesco, M., Long, J.A., and Weigel, D. (2010). On reconciling the interactions between APETALA2, miR172 and AGAMOUS with the ABC model of flower development. Development **137:** 3633–3642.

Würschum, T., Gross-Hardt, R., and Laux, T. (2006). APETALA2 regulates the stem cell niche in the *Arabidopsis* shoot meristem. Plant Cell **18:** 295–307.

Yant, L., Mathieu, J., Dinh, T.T., Ott, F., Lanz, C., Wollmann, H., Chen, X.M., and Schmid, M. (2010). Orchestration of the floral transition and floral development in *Arabidopsis* by the bifunctional transcription factor APETALA2. Plant Cell **22:** 2156–2170.

Yoshida, H., and Nagato, Y. (2011). Flower development in rice. J. Exp. Bot. **62:** 4719–4730.

Zhang, L.B., Zhu, Q.H., Wu, Z.Q., Ross-Ibarra, J., Gaut, B.S., Ge, S., and Sang, T. (2009). Selection on grain shattering genes and rates of rice domestication. New Phytol. **184:** 708–720.

Zhu, B.F., et al. (2011). Genetic control of a transition from black to straw-white seed hull in rice domestication. Plant Physiol. **155:** 1301–1311.

Zhu, Q.H., Upadhyaya, N.M., Gubler, F., and Helliwell, C.A. (2009). Over-expression of miR172 causes loss of spikelet determinacy and floral organ abnormalities in rice (*Oryza sativa*). BMC Plant Biol. **9:** 149–161.

Genetic Control of Seed Shattering in Rice by the APETALA2 Transcription Factor *SHATTERING ABORTION1*

Yan Zhou, Danfeng Lu, Canyang Li, Jianghong Luo, Bo-Feng Zhu, Jingjie Zhu, Yingying Shangguan, Zixuan Wang, Tao Sang, Bo Zhou and Bin Han

Plant Cell 2012;24;1034-1048; originally published online March 9, 2012;
DOI 10.1105/tpc.111.094383